Reaction of I_2 with the (001) surfaces of GaAs, InAs, and InSb. II. Ordering of the iodine overlayer

P. R. Varekamp
Department of Physics, Materials Physics, Royal Institute of Technology S-100 44 Stockholm, Sweden

M. C. Håkansson
Department of Synchrotron Radiation Research, Institute of Physics, Lund University, Sölvegatan 14, S-223 62 Lund, Sweden

J. Kanski
Department of Physics, Chalmers University of Technology, S-412 96 Göteborg, Sweden

M. Björkqvist and M. Göthelid
Department of Physics, Materials Physics, Royal Institute of Technology S-100 44 Stockholm, Sweden

B. J. Kowalski
Institute of Physics, Polish Academy of Sciences, 02-668 Warszawa, Poland

Z. Q. He
Department of Physics, Chalmers University of Technology, S-412 96 Göteborg, Sweden

D. K. Shuh* and J. A. Yarmoff
Department of Physics, University of California, Riverside, California 92521
and Materials Sciences Devision, Lawrence Berkeley National Laboratory, Berkeley, California 94720

U. O. Karlsson
Department of Physics, Materials Physics, Royal Institute of Technology S-100 44 Stockholm, Sweden
(Received 11 October 1995)

The overlayer formed by the reaction of molecular iodine (I_2) with GaAs(001), InAs(001), and InSb(001) is investigated with synchrotron soft x-ray photoelectron spectroscopy (SXPS) and scanning tunneling microscopy (STM). Two components, separated by about 0.5 eV, are present in all of the I 4*d* SXPS spectra. At very low iodine coverages, the high binding energy (BE) component dominates. When the iodine coverage saturates, however, the two components have nearly equal intensities. In contrast to GaAs and InAs, exposure of InSb(001)-$c(8\times2)$ to additional I_2 results in a further increase of the relative intensity of the low-BE component. STM images of I_2-covered InSb(001)-$c(8\times2)$ directly reveal the ordering in the overlayer. Islands are visible for submonolayer coverages, suggesting that adsorption occurs via a mobile precursor state. STM images collected from fully covered surfaces display two distinct types of atomiclike features. The predominant feature occupies a 1×1 unit cell with the same spacing as bulk-terminated InSb(001). The other feature has a coverage of $\sim1/3$ ML and is arranged in pairs oriented along the [110] azimuth. [S0163-1829(96)12527-3]

I. INTRODUCTION

This paper investigates the overlayers formed after reacting the GaAs(001)-$c(2\times8)$, GaAs(001)-$c(4\times4)$, InAs(001)-$c(8\times2)$, and InSb(001)-$c(8\times2)$ surfaces with molecular iodine (I_2). Synchrotron soft x-ray photoelectron spectroscopy (SXPS) and scanning tunneling microscopy (STM) are employed. SXPS is sensitive to the chemical state of an element, and thereby provides information about the bonding of surface species. This technique has been used previously to examine the overlayers formed on halogenated GaAs surfaces.[1–5] The images collected with STM display the real-space ordering of the surface, supplying both geometric and electronic surface structure information, STM has also been previously employed to image halogen overlayers formed on GaAs surfaces.[6–8]

In paper I, the interaction between I_2 and the (001) faces of GaAs, InAs, and InSb was investigated by examining changes in the substrate core-level spectra as a function of I_2 dose and sample anneal.[9] It was discovered that only the outermost element in the clean surface reconstruction shows significant reaction with iodine. All of the surfaces display a very strong 1×1 low-energy electron-diffraction (LEED) pattern after acquiring a saturation iodine coverage. This indicates that there is long-range order within the overlayer with a 1×1 unit cell that matches the lattice spacing of the bulk-terminated (001) substrate. Note that this order has also been investigated with angle-resolved photoemission.[10] Although all three substrates attain a saturation coverage of iodine, the reaction stops on GaAs and InAs, whereas further I_2 exposure etches InSb with a preferential loss of In.

The aim of the current paper is to explore the iodine overlayer itself. An SXPS analysis of the I 4*d* as a function of I_2 exposure and postannealing temperature reveals that the core level contains two distinct components at all times. This suggests the presence of two chemically inequivalent types of iodine. Since the overall behavior of the I 4*d* is quite similar for all of the surfaces studied, it is concluded that the overlayers all have similar structures. The dynamics of adsorption and the ordering within the overlayer are investigated via STM images collected from I_2-reacted InSb(001)-$c(8\times2)$. It is found that, at room temperature, I_2 diffuses via a mobile precursor state producing reacted islands on the surface. Two types of iodine are observed in high-resolution STM images collected from iodine-covered surfaces, but the present data cannot be used to conclusively conclude that these correspond to the two components in the I 4*d* spectra.

II. EXPERIMENTAL PROCEDURE

Although the experimental procedures are described in detail in Paper I, a brief synopsis is provided here. A solid-state electrochemical cell, which emits a collimated beam of molecular I_2, was used to dose the surfaces in ultrahigh vacuum (UHV).[11] Exposures were recorded in units of μA min, which represents the operating current of the cell integrated over the dosing time. It is preferable, however, to report the I_2 exposures in terms of a coefficient e, which is defined to be unity when the total amount of adsorbed iodine just saturates.[9] The iodine coverage for a particular exposure coefficient can then be found from the uptake curves presented in Paper I.

The synchrotron photoelectron spectroscopy was performed using the toroidal-grating monochromator beamline 41 at the MAX-lab Facility in Lund, Sweden.[12] The electron spectrometer is a goniometer-mounted hemispherical analyzer with an angular resolution of 2°. The total (photon plus electron) energy resolution was better than 0.2 eV. The In-rich $c(8\times2)$ reconstructions present on InAs(001) and InSb(001) were prepared by cycles of sputtering with Ar^+ ions and radiative annealing. The As-rich GaAs(001)-$c(2\times8)$ and -$c(4\times4)$ surfaces were prepared in a molecular-beam epitaxy (MBE) system attached directly to the beamline.

The STM images were collected using a commercial Omicron instrument in UHV (base pressure 3×10^{-11} mbar). The InSb(001) wafers were attached to a Ta sample holder via Ta foil spot-welded around the sample edges. The $c(8\times2)$ surfaces were prepared by several sputtering and annealing cycles. The samples were sputtered with 500-eV Ar^+ ions, at an angle of 45° with respect to the surface normal along the [110] azimuth, and then annealed to 350–400 °C. Surfaces prepared in this way contained large flat terraces on the order of 500 Å×1000 Å. All images are of filled states, and were collected in constant current mode with the sample biased at a selected voltage. Line scans were used to determine the height differences and lateral distances between various features.

III. RESULTS

A. I 4*d* core-level spectra

Figures 1 and 2 present an overview of the changes in the I 4*d* core level for the GaAs(001)-$c(2\times8)$, InAs(001)-$c(8\times2)$, and InSb(001)-$c(8\times2)$ surfaces, as a function of I_2 exposure and postannealing temperature. The I 4*d* core levels collected from the I_2-dosed GaAs(001)-$c(4\times4)$ surface are not pictured, as they are nearly identically to those collected from GaAs(001)-$c(2\times8)$. Effects due to band bending are removed by plotting the spectra relative to the valence-band maximum. This was accomplished by assigning constant binding energies (BE's) of As $3d_{5/2}$=40.47 eV, As $3d_{5/2}$=40.5 eV, and Sb $4d_{5/2}$=31.63 eV to the bulk core-level components in GaAs, InAs, and InSb, respectively.[13] Two components are clearly seen in the I 4*d* raw data for nearly all of the spectra shown. Due to the large spin-orbit splitting, these two components often produce four peaks in the raw data.

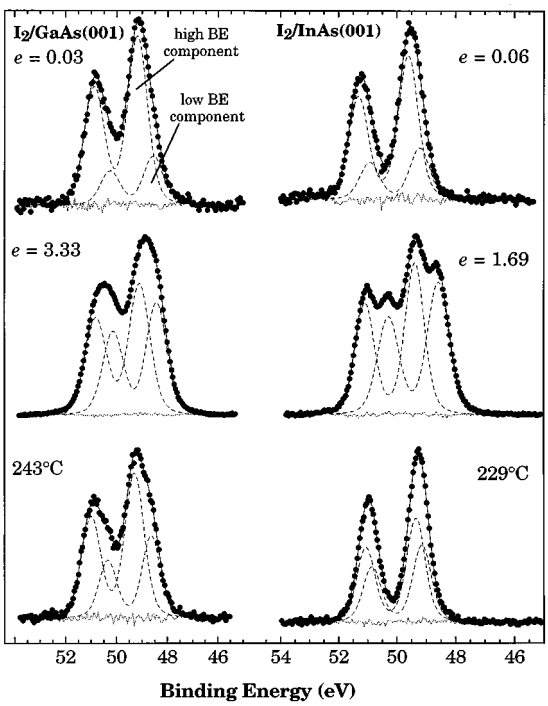

FIG. 1. High-resolution I 4*d* spectra, collected in normal emission with a photon energy of 90 eV, of I_2-reacted GaAs(001)-$c(2\times8)$ and InAs(001)-$c(8\times2)$ surfaces, together with the results of a numerical fitting procedure. The upper panels represent very low I_2 doses, the middle panels show the saturated surfaces, and the lower panels depict the final stages of annealing. The raw data, after background subtraction, are shown by filled circles, the individual fit components by dashed lines, the total fit result by a solid line, and the fit residuals by a dotted line. The binding energy scale is relative to the valence-band maximum.

The results of a numerical fitting procedure are also shown in Figs. 1 and 2. The I 4*d* core levels were fit to two spin-orbit split Gaussian-broadened Lorentzian doublets and a third-order spline background. The spin-orbit splitting and the Lorentzian width were fixed at 1.71 and 0.25 eV, respectively, for all fits in this paper. These values are consistent with previous treatments in the literature.[14,15] The branching ratios of the components within a given spectrum were never found to differ by more than 10%. As a further aid to finding appropriate numerical fits, spectra collected in normal emission were compared to spectra collected in at least one other

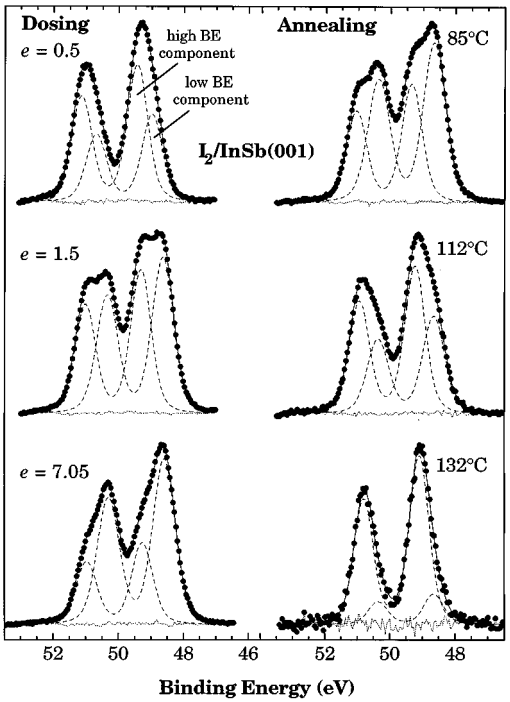

FIG. 2. High-resolution I 4*d* core-level spectra, collected in normal emission with a photon energy of 90 eV, of I_2-reacted InSb(001)-$c(8\times2)$ shown as a function of exposure and postanneal, together with the results of numerical fits. The legend for the symbols is the same as in Fig. 1. The binding-energy scale is relative to the valence-band maximum.

angle, usually 60° from the surface normal. Constraining the peak positions to be invariant with emission angle allowed for a more accurate determination of the fit parameters.

The general behavior of the I 4*d* spectra collected from all of the surfaces can be summarized as follows. After very small I_2 doses, the I 4*d* is composed primarily of a single component, with a very weak contribution from a second component at lower BE. As the surface is dosed with additional I_2, the relative intensity of the low-BE component increases. When the coverage of iodine reaches saturation, the two components each contribute 50 ± 5 % of the core-level area. Note, however, that the two components may reach equal intensity before the amount of iodine on the surface saturates. When the surface iodine is removed by annealing, the relative intensity of the low-BE component decreases. Thus, the intensity of the low-BE component increases more slowly upon adsorption and decreases more rapidly upon annealing, as compared with the intensity of the high-BE component.

The quantitative changes of the component intensities, summarized in the upper panels of Figs. 3 and 4, reveal that the only major difference in the behavior of the I 4*d* on the various surfaces occurs after large I_2 doses, i.e., for $e>1$. As shown in the top panels of Fig. 3, the relative intensities of the two components on GaAs(001) and InAs(001) are constant after a certain exposure. In contrast, on the InSb(001) surface, the relative intensity of the low-BE component continues to increase, as shown in the top-left panel of Fig. 4. After the largest I_2 exposure employed on InSb(001), the low-BE component contributed ~67% of the total I 4*d* area.

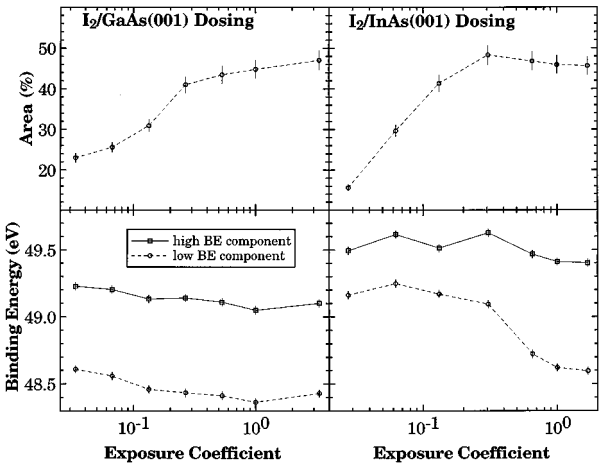

FIG. 3. Results of numerical fits to the I 4*d* core levels collected from GaAs(001)-$c(2\times8)$ and InAs(001)-$c(8\times2)$ as a function of I_2 exposure. The *x* axes are given on a log scale and are labeled with the exposure coefficient (see text). The top panels show the percent contribution of the low-BE component to the I 4*d*, while the bottom panels display the $4d_{5/2}$ binding energy of each component relative to the valence-band minimum.

Another general behavior of the I 4*d* level with I_2 dose is a monotonic decrease in the BE's of the two components. This is plotted in the lower panels of Figs. 3 and 4. The decrease in BE is attributed to an increase in final-state screening of the core holes as the surface becomes covered with iodine. Similar behavior has been observed for the I 4*d* level when Si(111) is exposed to I_2.[14] Note that the BE decrease is slightly different for the two I 4*d* components, which suggests that the amount of screening may be different for the species that give rise to the two components.

Figure 5 presents the changes in the I 4*d* as a function of electron emission angle for the iodine-covered InAs(001)-

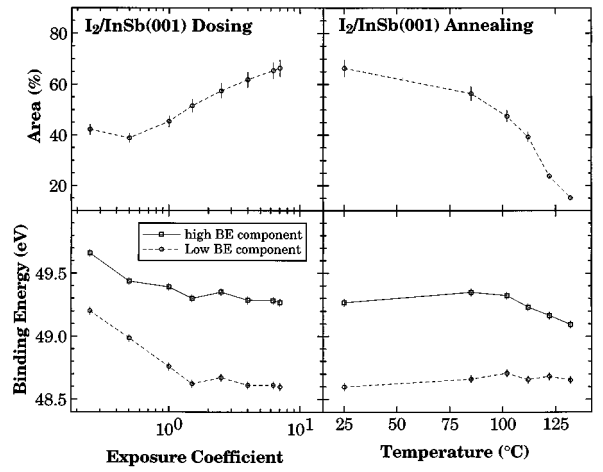

FIG. 4. Results of numerical fits to the I 4*d* core levels collected from InSb(001)-$c(8\times2)$ as a function of I_2 exposure and postanneal. The *x* axis in the dosing stage is given on a log scale and is indicated by the exposure coefficient (see text). The top panels show the percent contribution of the low-BE component, while the bottom panels display the $4d_{5/2}$ binding energy of each component relative to the valence-band minimum.

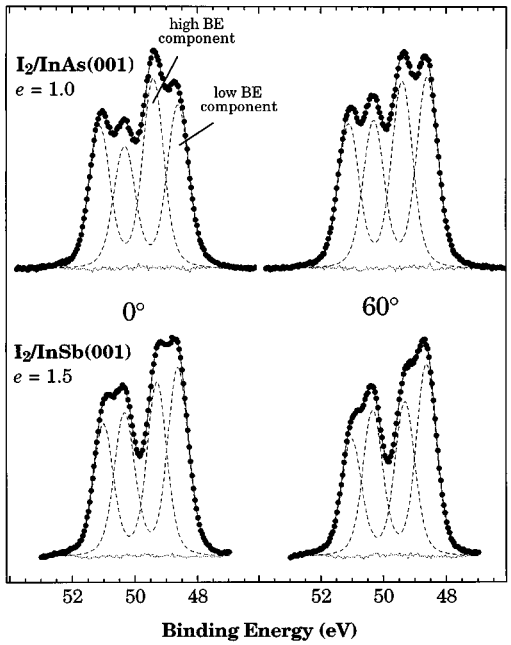

FIG. 5. High-resolution I 4*d* spectra collected at a 90-eV photon energy from iodine-covered InAs(001)-$c(8\times2)$ and InSb(001)-$c(8\times2)$, together with the results of numerical fits. The legend for the symbols is the same as in Fig. 1. The binding-energy scale is relative to the valence-band maximum. The spectra on the left (right) were collected for a 0° (60°) electron emission angle. The I_2 exposures for InAs(001) and InSb(001) were 288 μA min and 800 μA min, respectively.

$c(8\times2)$ and InSb(001)-$c(8\times2)$ surfaces. These spectra, which were collected along the [110] azimuth, show that there is a ~15% increase in the intensity of the low-BE component when the core level is collected off-normal. The relative intensity changes of the two components are attributed to a combination of diffraction and probing depth effects, and give additional evidence that each component is related to an arrangement of iodine on the surface. Some azimuthal dependence of the polar angle intensity variations was also observed. Such an azimuthal dependence can only occur if the overlayer is well ordered, which agrees with the LEED behavior discussed in Paper I,[9] and the STM results presented below.

B. STM images of I_2-reacted InSb(001)-$c(8\times2)$

Four STM images, collected from clean InSb(001)-$c(8\times2)$ and after reacting the surface with I_2, are shown in Fig. 6. Each image is 250 Å×250 Å and was collected from a different area of the surface. The images display variations in the tunneling current from filled electronic states, since they were collected with the sample biased negatively relative to the STM tip. Note that the most stable tunneling conditions were achieved with very low tunneling currents, i.e., when the tip was as far from the surface as possible for any given tunneling voltage. This was especially true when the surface was fully covered with iodine. It was found that subsequent imaging over the same part of the surface resulted in no significant changes to the images, which suggests that the features observed are independent from the action of the

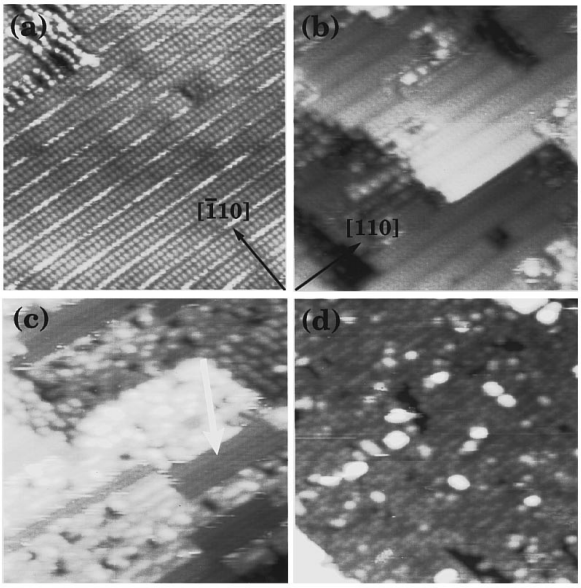

FIG. 6. Filled-state STM images of clean and I_2-dosed InSb(001). All panels are equally sized and show a 200 Å×200 Å area. Panel (a) depicts the clean InSb(001)-$c(8\times2)$ surface. The other images were collected after I_2 doses of (b) 25 μA min, (c) 70 μA min, and (d) 220 μA min. The sample bias and tunneling current for each image are (a) −1.1 V, 1.49 nA, (b) −2.0 V, 0.04 nA, (c) −1.6 V, 0.05 nA, (d) −2.2 V, 0.04 nA. The crystal axes appropriate for all the images are indicated. The arrow in (c) points to an area of unreacted double rows, such as seen in (a).

STM tip. This is in contrast to STM work performed on GaAs(110) exposed to Br_2 and Cl_2, where it was found that some halogen features were mobile, and could change following the acquisition of an image.[7]

The image in panel (a) of Fig. 6 was collected from the clean sputtered and annealed InSb(001)-$c(8\times2)$ surface. This image is dominated by paired rows of spots extending in the [110] azimuth. The distance between the spots in the [110] direction is, on average, 4.6 Å, which agrees with the surface lattice constant of InSb(001). This surface is judged to be typically clean and well ordered, as the above observations agree with previously published STM work on InSb(001).[16–19] Note, however, that in Refs. 16–19, the surface crystal axes are defined 90° perpendicular to the conventions used here.

Since the STM and photoemission experiments were not conducted in the same chamber, the exposures from the electrochemical cell cannot be compared directly. It was found, however, that the I_2 exposure required to completely cover the InSb surface, as judged by STM, was approximately 220 μA min, which is quite close to the 288 μA min that defined $e=1$ from SXPS. This suggests that the chamber geometry did not play a large role in the I_2 exposures, as would be expected for a cell that produces a collimated beam. Thus, approximate exposure coefficients are given below, so that the STM and SXPS data can be compared more readily.

Figure 6(b) shows an STM image obtained after exposing InSb(001)-$c(8\times2)$ to 25 μA min of I_2, i.e., $e\sim0.1$. This image contains predominantly two terraces, with some higher and lower terraces also visible. The height difference between the terraces is measured to be 3.2 Å, consistent with

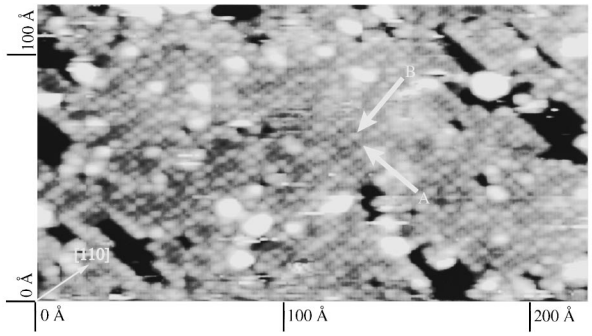

FIG. 7. Filled-state STM image of the InSb(001) surface after exposure to 320 μA min of I_2. This 130 Å×250 Å image was collected with a constant tunneling current of 0.09 nA, after biasing the sample −2.2 V relative to the tip. Arrows indicate the two basic types of spots present in the image: spots possessing a 1×1 symmetry labeled *A*, and paired spots labeled *B*.

the thickness of one In-Sb double layer. Very little reaction has occurred at this point, where reaction is defined to be a disruption of the double rows representing the $c(8\times2)$ reconstruction. Note, however, that the double rows have a different appearance than in panel (a), due to a difference in tunneling conditions.

The STM image shown in panel (c) was collected after the surface had been exposed to approximately three times the amount of I_2 as in Fig. 6(b). Nearly all of the surface shows obvious signs of reaction, but small patches do exist that contain the double rows indicative of the clean surface reconstruction, as indicated by the white arrow. The unreacted areas are always separated from the reacted areas by sharp, straight boundaries in both the [110] and [110] directions. This suggests that I_2 diffuses along the surface in a mobile precursor state before reacting. The presence of precursor state kinetics has been suggested previously for the adsorption of I_2 on this surface.[20]

The diffusion of I_2 on the InSb(001) surface can be contrasted to reactions of other halogens with III-V semiconductors. STM images collected after exposing GaAs(110) to Br_2 indicate that the diffusion length before reaction is significantly smaller at room temperature than in the present case.[7] This can be concluded from the relatively smaller size of the reaction islands and the more random distribution of reacted areas on the surface. An increase in the diffusion length does seem to occur when GaAs(110) is dosed with Br_2 above room temperature, however.

The STM image in Fig. 6(d) displays the InSb(001) surface after it has been fully covered by reacted areas, i.e., for $e\sim1$. The first observation that can be made from this image is that the surface appears smoother and more homogeneous than the reacted areas visible in panels (b) and (c). Another characteristic trait of the image in Fig. 6(d) is the presence of pairs of spots, oriented along the [110] azimuth, that are ''brighter'' than the surrounding substrate.

When the surface is reacted with additional I_2, the pairs of bright spots, which are indicated by arrow *B* in the close-up image of Fig. 7, remain visible. The I_2 exposure for this image corresponds to $e\sim1.3$. A closer examination of the image reveals that the areas between the bright pairs of spots are also composed of spots, illustrated by arrow *A*, which are slightly darker than the paired spots. Distance measurements

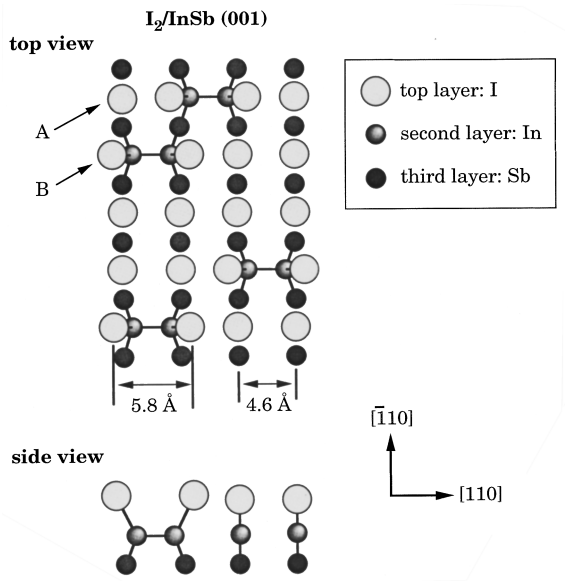

FIG. 8. Atomic-scale schematic diagram of the iodine-covered InSb(001) surface illustrating a possible arrangement of iodine atoms which is consistent with the STM, SXPS, and LEED data. Two different adsorption sites are depicted: *A*, iodine bonded atop an In atom after breaking the In-In dimer bond, and *B*, iodine bonded to an In atom in an unbroken dimer.

performed via line scans of this image show that the type *A* spots are spaced 4.6 Å apart in both the [110] and [110] directions, which agrees with a 1×1 unit cell on a InSb(001) surface. The two spots in a bright pair, i.e., type-*B* spots, are found to be ~25% farther apart in the [110] azimuth, i.e., separated by ~5.8 Å. Assuming that each type-*B* spot represents a single atom, the coverage is estimated to be 0.37 ±0.06 ML, or slightly over $\frac{1}{3}$ ML. The height difference between the *A* and *B* spots is typically 0.4 Å, as measured in line scans taken from the image shown in Fig. 7.

The following analysis suggests that both spots of types *A* and *B* observed in the STM images are, indeed, associated with adsorbed iodine. The strong 1×1 LEED pattern observed from this surface indicates that the iodine in the overlayer is ordered with the same periodicity as the bulk-terminated InSb(001) 1×1 unit cell. Thus, the ordering of the *A* spots in 1×1 sites is good evidence that they represent iodine atoms. Such an explanation is not applicable for the $\frac{1}{3}$ ML of *B* spots, however, which are not located in 1×1 sites, and would thus contribute only to the LEED background. It is likely, however, that the *B* spots do represent iodine atoms, and not, for example, filled lone-pair orbitals. Bright pairs of spots have been observed in STM images of clean InSb(001)-$c(8\times2)$ [see, for example, Fig. 6(a)] and have been explained as filled lone-pair orbitals of second-layer Sb atoms.[16–18] This explanation is not applicable for the type-*B* spots, however, since the pairing observed in the filled-state images shown here occurs in an azimuthal direction that is 90° from the direction of the Sb lone-pair orbitals. If both type-*A* and *B* spots are iodine atoms, it is then clear that the surface coverage is 1.0 ML, since there is one spot at each 1×1 surface site.

One possible interpretation of the type-*B* spots is that they image iodine atoms bound to unbroken In dimers. A diagram of such a surface atomic structure is given in Fig. 8. Note

that the atomic arrangement shown is based on the diagram in Fig. 7(c) of Paper I for the saturated surface,[9] with the added complexity that some of the surface dimers are not broken. The main support for this argument is that the type-*B* spots are paired, and always point along the [110] azimuth, which is the same direction as the In dimers on the clean $c(8\times2)$ surface.[17,18,21] Furthermore, the distance between the *B* spots in a pair is slightly larger than the unreconstructed 1×1 distance, which might be expected for iodine bonded to an unbroken dimer. This idea implies that I_2 breaks only about $\frac{2}{3}$ of the surface dimers upon reaction. Note that the In 4*d* BE may also be different for InI formed at broken or unbroken dimers. It is likely, however, that this difference is not resolvable in the In 4*d* spectra presented in Paper I.

A general statement that can be made regarding the behavior of iodine on the InSb(001) surface is that rearrangements occur within the overlayer as the sample is exposed to I_2 and is subsequently annealed. This is seen clearly in the STM images, which show a transition between a surface with iodine islands possessing no obvious internal order, to a completely covered homogeneous surface that has both long- and short-range order. Rearrangements within the overlayer are also suggested by the changes that occur in the I 4*d* core level as a function of exposure and annealing. Although STM images were only collected for InSb(001), the similarity in the I 4*d* core levels presented here, and the LEED and SXPS measurements presented in Paper I,[9] implies that the iodine overlayer behavior is basically the same on all of the III–V substrates. In fact, rearrangements within an iodine overlayer as a function of coverage are commonly observed on metal surfaces, and have been attributed to I-I interactions.[22–24]

IV. DISCUSSION

The exact source of the two components in the I 4*d* core level is a perplexing problem. The fact that two components are seen on all the surfaces, and that their intensities are approximately equal when the coverage of iodine saturates, suggests that there is an underlying fundamental behavior. This fundamental behavior may also be the same as is exhibited by Br_2 on GaAs(110), since two Br 3*d* components are also observed in approximately equal proportions.[2] Note that two components are also seen in the Cl 2*p* core level collected from GaAs surfaces exposed to Cl_2, although, in that case, the origin appears to be different.[4,25]

One statement that can be made with certainty is that the two I 4*d* components are not due to iodine bonding to group-III vs -V elements. A general conclusion reached in Paper I was that iodine reacts predominantly with the outermost element on the surface.[9] Yet, the I 4*d* spectra collected from all the surfaces reveal two equal components, regardless of the surface termination. Perhaps the most striking evidence in support of this is given by the behavior of the GaAs(001)-$c(4\times4)$ surface. This very As-rich surface is thought to have no exposed Ga atoms,[26–28] and the substrate core-level fits reported in Paper I for the I_2-saturated surface do not display any measurable bonding between iodine and gallium.[9] At the same time, however, the I 4*d* level has two nearly equal intensity components. The conclusion that the two components are not due to group-III vs -V element bonding was also reached for Br 3*d*, via a comparison to the proportions of different bonding sites in STM images.[7]

It is quite possible that there is some relationship between the two different species observed in STM on iodine-covered InSb(001) and the two I 4*d* components, but there is no conclusive evidence. The proportion of the two species observed in STM does not correspond exactly with the nearly equal intensities of the two components in the I 4*d* at $e=1$. However, 15% changes can occur due to electron diffraction, as shown by Fig. 5, which could account for this difference. Also, since only a rough correspondence can be made between the exposures in the SXPS and STM experiments, it is difficult to know which image should be compared with which I 4*d* spectrum. Furthermore, the proportions of the two I 4*d* components change for exposures above $e=1$ for InSb, which is likely related to the etching that occurs with this surface.[9] STM measurements of the iodine overlayers formed on other III-V semiconductors would be very enlightening.

The possibility that iodine molecules exist on the surface, as was suggested previously for the reaction between I_2 and GaAs(001),[29] must also be considered. Molecules on the surface could manifest themselves as two I 4*d* components in two different ways. One, the adsorption of iodine could be molecular at all coverages, with each molecule possessing two inequivalent atoms, for example, if they were bonded perpendicular to the surface. Alternatively, a coexistence of molecules and atoms on the surface may result in two I 4*d* components. Note that a change from atomic to molecular adsorption was observed previously for I_2 reacted with Fe surfaces at low temperatures, although, in that case, the adsorption only becomes molecular after all of the vacant metal sites on the surface are tied up with atomic I.[30]

Although the presence of molecules on the surface cannot be ruled out, there is no other support for their existence in the current data. For example, in the STM image in Fig. 7, the pairing of the type-*B* spots cannot represent I_2 molecules lying flat on the surface, since an I-I bond length is much shorter, varying from 2.662 Å for gaseous I_2 to 2.715 Å in solid I_2.[31] Further attempts have been made to prove the existence of molecules or lack thereof. For example, an ~4-eV energy loss attributed to molecular iodine has been observed on metal surfaces via electron energy-loss spectroscopy.[32] Attempts to observe this loss from I_2-saturated GaAs(001)-4×6 were inconclusive, however.[33] Preliminary low-energy ion-scattering studies of I_2-saturated GaAs(001)-4×6 have also been performed, which concluded that if any I_2 does exist on the surface, its molecular axis is not directed perpendicular to the surface.[33] A more conclusive way to determine the presence or absence of adsorbed molecules would be to perform vibrational studies of the surface species.

The most likely explanation, therefore, is that iodine adsorbs dissociatively at all coverages, and that the two components in the I 4*d* are due to two different adsorption sites. This explanation could apply equally well to the two Br 3*d* components observed on brominated GaAs(110).[2] The behavior of the I 4*d* components with I_2 exposure indicates that there is a preference for populating the site corresponding to the high-BE component at low coverages, and that the pref-

erence gradually switches to the other site as the coverage increases. The site corresponding to the high-BE component cannot fill completely before the other site is populated, however, since every I $4d$ spectrum possessed two components, even those collected after the lowest doses. This is probably due to the fact that islands form even at very low coverages, so that, locally, the high-BE site can become fully populated after very low exposures. Also, note that the rapid decrease in the intensity of the low-BE component after light annealing may not be due to the same mechanism as its rapid increase with I_2 exposure. Iodine is not simply desorbing from the surface in all cases, but is sometimes carrying substrate material with it.[9]

V. SUMMARY

The behavior of the I $4d$ core level on four III-V (001) surfaces was studied as a function of I_2 dose and sample anneal. Two components are seen at all coverages. The relative intensity of the low-BE component increases more slowly as a function of exposure, and decreases more rapidly when the surface is heated. STM images of the InSb(001)-$c(8\times2)$ surface following I_2 dose show island formation, and hence evidence of diffusion via a mobile precursor state before reaction. When the surface is completely covered, the ordered overlayer possesses two types of features. The darker features correspond to a 1×1 lattice spacing of the InSb substrate. The brighter features are always found in pairs oriented in the [110] direction and spaced slightly farther apart than the bulk InSb(001) lattice spacing. More work is needed, however, in order to ascertain the relationship between the two I $4d$ components and the features observed in the STM images.

ACKNOWLEDGMENTS

The financial support of the Swedish Natural Science Research Council and NUTEK through the Nanometer Structure Consortium is gratefully acknowledged. J.A.Y. acknowledges the U.S. Army Research Office for partial support.

*Present address: Chemical Sciences Division, Lawrence Berkeley National Laboratory, Berkeley, CA 94720.

[1] A. B. McLean, L. J. Terminello, and F. R. McFeely, Phys. Rev. B **40**, 11 778 (1989).
[2] C. Gu, Y. Chen, T. R. Ohno, and J. H. Weaver, Phys. Rev. B **46**, 10 197 (1992).
[3] R. D. Schnell, D. Rieger, A. Bogen, K. Wandelt, and W. Steinmann, Solid State Commun. **53**, 205 (1985).
[4] D. K. Shuh, C. W. Lo, J. A. Yarmoff, A. Santoni, L. J. Terminello, and F. R. McFeely, Surf. Sci. **303**, 89 (1994).
[5] F. Stepniak, D. Rioux, and J. H. Weaver, Phys. Rev. B **50**, 1929 (1994).
[6] F. Osaka, T. Ishikawa, N. Tanaka, and M. Lopez, J. Vac. Sci. Technol. B **12**, 2894 (1994).
[7] J. C. Patrin and J. H. Weaver, Phys. Rev. B **48**, 17 913 (1993).
[8] J. C. Patrin, Y. Z. Li, M. Chander, and J. H. Weaver, Appl. Phys. Lett. **62**, 1277 (1993).
[9] P. R. Varekamp, M. C. Håkansson, J. Kanski, D. K. Shuh, M. Björkqvist, M. Göthelid, W. C. Simpson, U. O. Karlsson, and J. A. Yarmoff, preceding paper, Phys. Rev. B **54**, 2101 (1996).
[10] P. R. Varekamp, M. C. Håkansson, J. Kanski, B. J. Kowalski, L. Ö. Olsson, L. Ilver, Z. Q. He, J. A. Yarmof and U. O. Karlsson, Surf. Sci. **352–354**, 387 (1996).
[11] N. D. Spencer, P. J. Goddard, P. W. Davies, M. Kitson, and R. M. Lambert, J. Vac. Sci. Technol. A **1**, 1554 (1983).
[12] U. O. Karlsson, J. N. Andersen, K. Hansen, and R. Nyholm, Nucl. Instrum. Methods A **282**, 553 (1989).
[13] *Electronic Structure of Solids: Photoemission Spectra and Related Data*, edited by A. Goldman and E.-E. Koch, Landolt-Börnstein, New Series, Group III, Vol. 23, Pt. a (Springer, Berlin, 1989).
[14] V. Chakarian, D. K. Shuh, J. A. Yarmoff, M. C. Håkansson, and U. O. Karlsson, Surf. Sci. **296**, 383 (1993).
[15] S. Söderholm, B. Loppinet, and D. Schweitzer, Synth. Met. **62**, 187 (1994).
[16] C. F. McConville, T. S. Jones, F. M. Leibsle, and N. V. Richardson, Surf. Sci. **303**, L373 (1994).
[17] C. F. McConville, T. S. Jones, F. M. Leibsle, S. M. Driver, T. C. Q. Noakes, M. O. Schweitzer, and N. V. Richardson, Phys. Rev. B **50**, 14 965 (1994).
[18] M. O. Schweitzer, F. M. Leibsle, T. S. Jones, C. F. McConville, and N. V. Richardson, Surf. Sci. **280**, 63 (1993).
[19] M. O. Schweitzer, F. M. Leibsle, T. S. Jones, C. F. McConville, and N. V. Richardson, Semicond. Sci. Technol. **8**, S342 (1993).
[20] A. P. Mowbray and R. G. Jones, Vacuum **41**, 672 (1990).
[21] P. John, T. Miller, and T.-C. Chiang, Phys. Rev. B **39**, 1730 (1989).
[22] D. R. Mueller, T. N. Rhodin, Y. Sakisaka, and P. A. Dowben, Surf. Sci. **250**, 185 (1991).
[23] N. R. Avery, J. Appl. Phys. Suppl. 2, Pt. 2, 193 (1974).
[24] N. R. Avery, Surf. Sci. **43**, 101 (1974).
[25] W. C. Simpson, D. K. Shuh, W. H. Hung, M. C. Håkansson, J. Kanski, U. O. Karlsson, and J. A. Yarmoff, J. Vac. Sci. Technol. A (to be published).
[26] P. K. Larsen, J. H. Neave, J. F. van der Veen, P. J. Dobson, and B. A. Joyce, Phys. Rev. B **27**, 4966 (1983).
[27] J. F. van der Veen, P. K. Larsen, J. H. Neave, and B. A. Joyce, Solid State Commun. **49**, 659 (1984).
[28] D. K. Biegelsen, R. D. Bringans, J. E. Northrup, and L.-E. Swartz, Phys. Rev. B **41**, 5701 (1990).
[29] P. R. Varekamp, M. C. Håkansson, D. K. Shuh, J. Kanski, L. Ilver, Z. Q. He, J. A. Yarmoff, and U. O. Karlsson, Vacuum **46**, 1231 (1995).
[30] D. Mueller and T. N. Rhodin, Surf. Sci. **164**, 271 (1985).
[31] F. van Bolhuis, P. B. Koster, and T. Migchelsen, Acta Crystallogr. **23**, 90 (1967).
[32] P. A. Dowben, M. Grunze, and S. Varma, Solid State Commun. **57**, 631 (1986).
[33] C. B. Weare, T.-Y. Liu, and J. A. Yarmoff (unpublished).